

## Charge exchange spectroscopy by Fabry–Pérot spectrometer in W7-AS

M. Yoshinuma, K. Ida, and J. Baldzuhn

Citation: *Rev. Sci. Instrum.* **75**, 4136 (2004); doi: 10.1063/1.1789587

View online: <http://dx.doi.org/10.1063/1.1789587>

View Table of Contents: <http://rsi.aip.org/resource/1/RSINAK/v75/i10>

Published by the [American Institute of Physics](#).

---

### Related Articles

Ion pseudoheating by low-frequency Alfvén waves revisited  
*Phys. Plasmas* **20**, 012121 (2013)

Neutral beam heating of a RFP plasma in MST  
*Phys. Plasmas* **19**, 122505 (2012)

The effects of neutral gas heating on H mode transition and maintenance currents in a 13.56MHz planar coil inductively coupled plasma reactor  
*Phys. Plasmas* **19**, 093501 (2012)

Collisionless inter-species energy transfer and turbulent heating in drift wave turbulence  
*Phys. Plasmas* **19**, 082309 (2012)

Development of a low-energy and high-current pulsed neutral beam injector with a washer-gun plasma source for high-beta plasma experiments  
*Rev. Sci. Instrum.* **83**, 083504 (2012)

---

### Additional information on Rev. Sci. Instrum.

Journal Homepage: <http://rsi.aip.org>

Journal Information: [http://rsi.aip.org/about/about\\_the\\_journal](http://rsi.aip.org/about/about_the_journal)

Top downloads: [http://rsi.aip.org/features/most\\_downloaded](http://rsi.aip.org/features/most_downloaded)

Information for Authors: <http://rsi.aip.org/authors>

## ADVERTISEMENT

**JANIS** Does your research require low temperatures? Contact Janis today.  
Our engineers will assist you in choosing the best system for your application.



10 mK to 800 K      LHe/LN<sub>2</sub> Cryostats  
Cryocoolers      Magnet Systems  
Dilution Refrigerator Systems  
Micro-manipulated Probe Stations

[sales@janis.com](mailto:sales@janis.com)      [www.janis.com](http://www.janis.com)  
Click to view our product web page.

# Charge exchange spectroscopy by Fabry–Pérot spectrometer in W7-AS

M. Yoshinuma<sup>a)</sup> and K. Ida

*National Institute for Fusion Science, Toki 509-5292, Japan*

J. Baldzuhn

*MaxPlanck Institute for Plasma Physics, Wendelsteinstrasse, 1, 17491 Greifswald, Germany*

(Presented on 21 April 2004; published 13 October 2004)

Charge exchange spectroscopy using a Fabry–Pérot spectrometer has been developed to study the dynamic of ion temperature and radial electric field in plasmas. A charge coupled device detector with  $80 \times 80$  pixels was used to gain the spectral resolution of the charge exchange spectroscopy system. This Fabry–Pérot charge exchange spectroscopy system has been applied to measure the ion temperature using the charge exchange line of carbon impurity with a time resolution of 5 ms for high density quasisteady discharges in W7-AS. The cold component due to the charge exchange reaction between the carbon impurity and thermal neutrals is subtracted from the change emission with the beam modulation technique © 2004 American Institute of Physics.

[DOI: 10.1063/1.1789587]

## I. INTRODUCTION

Charge exchange spectroscopy (CXs) has been used to measure the profile of ion temperature and plasma rotation velocity in both the poloidal and toroidal direction in tokamak and helical plasmas.<sup>1,2</sup> An improvement of time resolution of the CXs has been desired eagerly as going to study the dynamic behaviors of radial electric field in the plasma where the radial electric field changes rapidly at the transition to the confinement improved mode or in the breathing phase. Since the background emissions from the charge exchange with the thermal neutrals around the peripheral of the plasma overlaps the charge exchange emission to be measured, the background emission should be subtracted from the charge exchange emission to derive local ion temperature. The beam modulation is one of the techniques to subtract the background emission. The improvement of the time resolution is also useful for the CXs measurement with the beam modulation. A Fabry–Pérot spectrometer has good spectral resolution, therefore the aperture for input light can be larger compared with the slit of a conventional spectrometer. Charge exchange spectroscopy using a Fabry–Pérot spectrometer was developed and installed in the JIPP TII-U tokamak. The spectral resolution was limited by the number of two dimensional (2D) photodiodes of the detector.<sup>3</sup> The 2D photodiodes array was replaced with the charge coupled device (CCD) image detector to improve the spectral resolution.

## II. CXS SYSTEM BY FABRY–PÉROT SPECTROMETER

Figure 1 shows the schematic view of the CXs system using Fabry–Pérot spectrometer. The system consists of an étalon with a spacing of  $75 \mu\text{m}$ , two optical lenses, one interference filter, CCD image detector, and a bundle of seven optical fibers that are arranged on an optical axis. The étalon

has 1.7 nm of free spectrum range (FSR) which is large enough to measure the Doppler broadened spectrum for the plasma with the ion temperature of 1 keV. The center wavelength and bandwidth of the interference filter are 529.1 and 1.5 nm, which is narrower than the FSR of the étalon to cut the interference of the higher order of spectrum, respectively. The carbon impurity line ( $\text{C VI } \lambda=529.1 \text{ nm}$ ) is used for the CXs measurement. Two optical lenses are arranged at each side of the étalon. The wavelength  $\lambda$  transmitting the étalon with the finite angle  $\theta_d$  are given by

$$\lambda_d = \lambda_0 \cos \theta_d = \lambda_0 (f / \sqrt{f^2 + d^2}), \quad (1)$$

where  $d, f, \theta_d$ , and  $\lambda_0$  are the distance from the optical axis, the focal length of the coupled lens, light injection angle into the étalon against the optical axis, and center wavelength transmitting the étalon along the optical axis. The system has six channels for measurement (Nos. 1–6 in Fig. 1) and one channel for calibration (No. 0 in Fig. 1) of center wavelength. The CCD detector is arranged at the focal plane of the lense opposite the fiber bundle. The back illumination CCD detector with  $80 \times 80$  pixels ( $36 \mu\text{m}$  pixel size) is used to increase quantum efficiency. The image of the aperture of the fiber bundle is focused on the CCD detector. The wavelength for each pixel is calculated from the distance of the pixel position from the optical axis by using formula (1).

## III. CALIBRATIONS OF FABRY–PÉROT SYSTEM

Figure 2 shows the spectra of the Sm and Cu lamps measured with the Czerny–Turner type spectrometer, which is already calibrated and the Fabry–Pérot system. Because the range of the wavelength of the Fabry–Pérot system, which is limited by a diameter of the optical fiber, is 0.8 nm the center wavelength of the étalon is tuned at 528.8 and 529.75 nm for Sm line and 529.75 and 530.45 nm for Cu line. The wavelengths in Fig. 2(b) are calculated with formula (1). The center wavelength of the étalon is calibrated

<sup>a)</sup>Electronic mail: yoshinuma@nifs.ac.jp

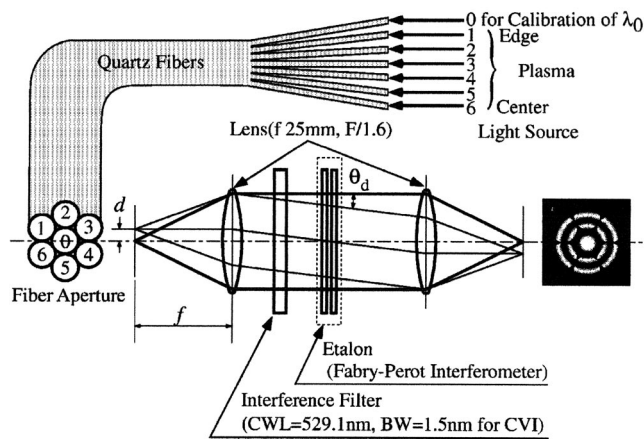


FIG. 1. Schematic view of the Fabry-Pérot CXS system.

by using the peak at 528.291 nm of the Sm lamp and at 529.25 nm of the Cu lamp. The spectrum, which was observed with the Czerny-Turner type spectrometer is almost identical to that observed with the Fabry-Pérot system.

Figures 3(a) and 3(b) show the spectrum of the Cu lamp (529.25 nm) without and with the intensity calibration, respectively. The intensity decreases as the distance from the optical axis is increased (away from the CCD center) as seen

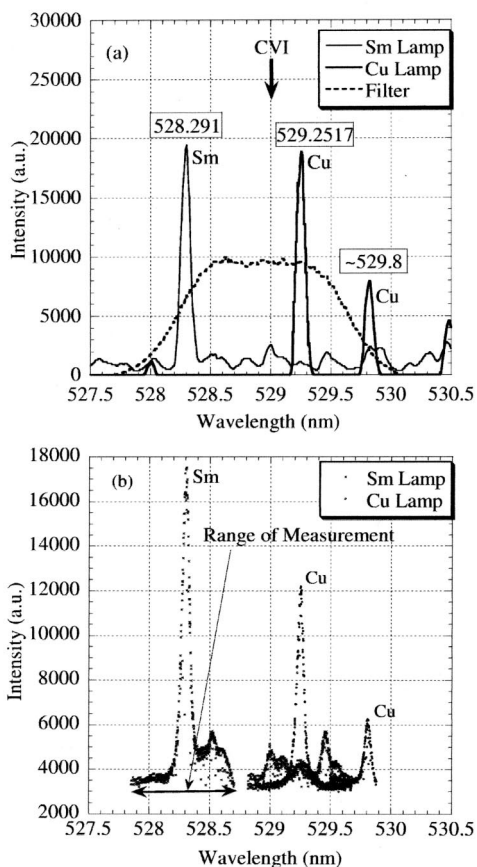


FIG. 2. Spectra of the Cu and Sm lamp measured by using the: (a) Czerny-Turner type spectrometer and (b) Fabry-Pérot spectrometer. Dotted line indicates the characteristic curve of the interference filter used for the Fabry-Pérot spectrometer. The arrow in (a) indicates the wavelength of the C VI line without Doppler shift. The arrow in (b) indicates the range of wavelength acquired with a fixed space of Fabry-Pérot interferometer.

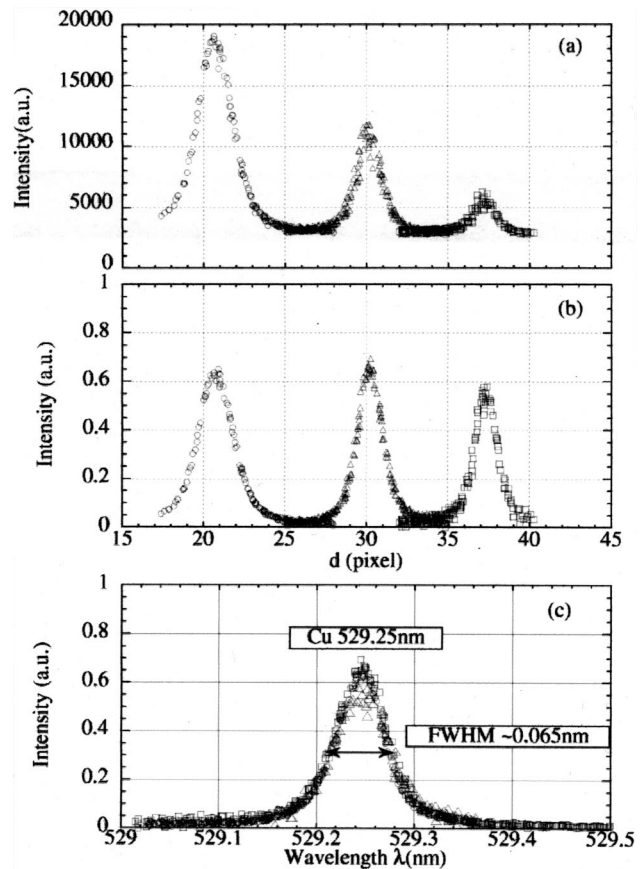


FIG. 3. Spectra of Cu (529.25 nm) measured at the inner (circle), middle (triangle), and outer (square) region of CCD image: (a) without intensity calibration, (b) without intensity calibration, and (c) with intensity calibration plotted on wavelength axis.

in Fig. 3(a). The light intensity at the center region of the image is higher than that at the outer region of the image because the effective aperture of the étalon for the outer region of the image is decreased. Furthermore the sensitivity of pixels of the CCD are scattered slightly. The profile of the photons throughput are measured by injecting the white light (halogen lamp) uniformly and is used for the intensity calibration. Figure 3(b) shows the spectra after the intensity is corrected with the calibration of throughput. The scatterings of the data are also corrected by the intensity calibrations and the  $\chi^2$  value of the fitting with Gaussian curve decreases to 1/3 compared with the data without the calibration.

Because the dispersion of the Fabry-Pérot system is not linear on  $d$ , the width of the spectra at the position is larger than that at the outer position. Figure 3(c) shows the spectrum of the Cu lamp (529.25 nm) plotted on the axis of the wavelength. The spectra measured at different  $d$  overlap each other. The instrumental width from full width half maximum (FWHM) of the spectrum is 0.065 nm. The wavelength resolution of the data points is about 0.0015 nm, which is much smaller than the instrumental width of the Fabry-Pérot spectrometer. The resolution of the Fabry-Pérot system is limited by the instrumental width. The instrumental width of 0.065 nm corresponds to 0.03 keV in the Doppler width of carbon impurity, which is much smaller than the target temperature of 1 keV. The effective finesse (FSR/FWHM)

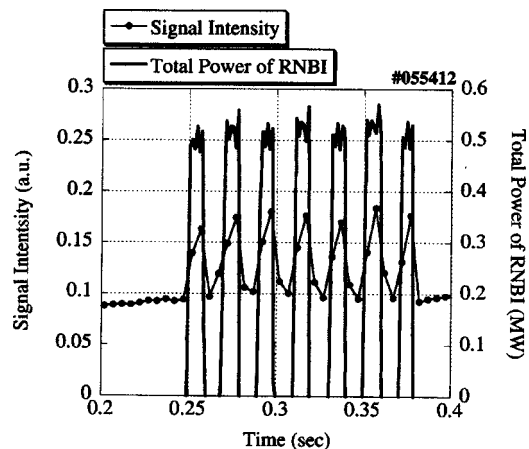


FIG. 4. Time evolution of signal intensity (circle) plotted with the total power of RNBI (solid line).

which indicates the performance of a Fabry–Pérot system is 26, while the Fabry–Pérot system installed in JIPP TII-U in 1995<sup>3</sup> was only 14.

#### IV. CXS MEASUREMENT IN W7-AS

The Fabry–Pérot system are installed in W7-AS with six line of sights which cross the neutral beam of the radial neutral beam injector (RNBI). The charge exchange line of carbon impurity is measured with a time resolution of 5 ms with exposure time 3.5 ms for high-density quasisteady discharge. The line averaged density is  $3.7 \times 10^{20} \text{ m}^{-3}$  and the total heating power of the neutral beam is 3.5 MW.

Figure 4 shows the time evolution of C VI intensity and the total power of the RNBI. The C VI intensity is modulated with 50 Hz associated with the modulation of the radial injector of the neutral beam (10 ms on, 10 ms off). The intensity of the charge exchange line due to the beam is comparable to the intensity induced by charge exchange reaction

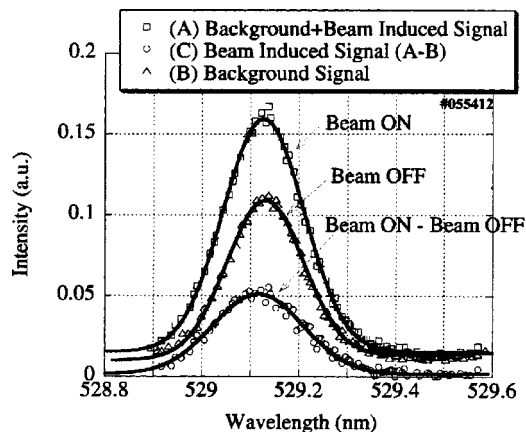


FIG. 5. Spectra of the charge exchange line of C VI with the RNBI on (open square), off (open triangle), and the beam induced component (open circle). Solid lines the curve of fitting with Gaussian profile.

between carbon and thermal neutrals (background).

Figure 5 shows the charge exchange spectrum of C VI at the timing of beam on (at 0.262 s) and beam off (at 0.267 s). The difference between the spectra at beam on and beam off gives C VI emission emitted from the cross section between line of sight and the neutral beam line. The ion temperature derived from the Doppler width after subtracting the background is 350 eV.

#### ACKNOWLEDGMENTS

The authors would like to thank the W7-AS team for their support of this work. This work is supported by a grant-in-aid for scientific research from MEXT, Japan.

<sup>1</sup>K. Ida, S. Kado, and Y. Liang, Rev. Sci. Instrum. **71**, 2360 (2000).

<sup>2</sup>J. Baldzuhn, W. Ohlendorf, and the W7-As-Team, Rev. Sci. Instrum. **68**, 1020 (1997).

<sup>3</sup>K. Ida, Fusion Eng. Des. **34–35**, 219 (1997).